e-ISSN 2320 –7876 www.ijfans.org
Vol.11, Iss.9, Dec 2022

Sol-gel combustion synthesis and characterization studies La doped $BiFeO_3$ nanoparticles

S. Peter Vijay [1,*], G. Veeramani [1], G. Padma Priya[1]
[1] Department of Chemistry, Faculty of Arts and Science,
Bharath Institute of Higher Education and Research (BIHER),
Chennai – 600073, Tamil Nadu, India
***Corresponding Author Email addresses: petervijy.solom@gmail.com (S. Peter Vijay)**

Address for Correspondence

S. Peter Vijay [1,*], G. Veeramani [1], G. Padma Priya[1]
[1] Department of Chemistry, Faculty of Arts and Science,
Bharath Institute of Higher Education and Research (BIHER),
Chennai – 600073, Tamil Nadu, India
***Corresponding Author Email addresses: petervijy.solom@gmail.com (S. Peter Vijay)**

Abstract

In this present work, $BiFeO_3$ (BFO) and $La_{0.05}Bi_{0.95}FeO_3$ (LBFO) nanoparticles have been synthesized using urea as a fuel via sol-gel combustion method. The synthesized materials have been analyzed by Powder X-ray diffraction (XRD), Fourier- Transform Infrared spectroscopy (FT-IR), Ultraviolet-visible (UV-Vis.) spectroscopy, High-resolution scanning electron microscopy (HR-SEM), HR-TEM, Magnetic measurements and antimicrobial studies. The X-ray diffraction patterns (XRD) of BFO demonstrates the rhombohedrally distorted perovskite structure with the space group R3c. Furthermore, the average particle size of BFO and LBFO were found to be 19 and 17nm respectively. The morphological studies of BFO and LBFO revealed the formation of sphere shaped nanostructures with uniform grain size. Also, it was found that the grain size was decreased by doping La contents to BFO. The magnetic measurements showed a ferromagnetic behavior of LBFO and the saturation magnetization drops drastically from 7 emu/g for $BiFeO_3$ up to 6 emu/g.

Keywords: $BiFeO_3$ nanoparticles; Urea*;* Sol-gel method; antibacterial activity.

1. Introduction

The ferrite materials are receiving much attention for their potential applications in various devices. The Bismuth ferrite ($BiFeO_3$) is the best promising material for various industrial

applications [1]. $BiFeO_3$ (BFO) possesses ABO_3 -type simple perovskite structure that shows multiferroic at room-temperature [2]. Moreover, the ferrite nanomaterials possess several properties like ferroelectricity, ferromagnetism, and ferroelasticity in single crystal [3,4] and can be used in multifunctional, low-power consumption, and environmentally friendly devices. In addition, BFO can also be used in photodegradation of organic dyes, wastewater treatments, air purification processes, photovoltaic and in water splitting for hydrogen production to generate clean energy [5-14].

There are certain dopant groups have been reported to increase the magnetic properties of BFO nanoparticles. By substituting either on the Bi site by trivalent rare-earth and divalent ions or on the Fe site by transition metal ions, the magnetic properties can be enhanced. It is found that the partial substitution of Bi by rare-earth (RE) ions may induce a ferromagnetic response, which has been ascribed to destruction of the spiral modulation.

In general, doping of the Bi^{3+} A site of the perovskite with RE cations has received extensive attention with a variety of symmetries, magnetic and electric behaviors.[15] Moreover, it is found that La-doped BFO films has enhanced ferroelectric remnant polarization and ferromagnetic properties [16]. Rare earth ferrites are widely used in biomedical sectors, ball bearings and hard face seals, oil drilling, automotive and marine engines, industrial machines, magneto-optical materials, magnetic refrigerant materials etc. [17]. The RE elements can facilitate the abruption of photogenerated electron-hole pairs because of their special 4f electron configurations and shows improved magnetic properties with increased stability of the material. Furthermore, BFO nanoparticles are used in the degradation and mineralization of dye pollutants. In this paper La doped BFO nanoparticles have been synthesized by sol-gel combustion method using urea as the fuel (reducing agent) [18].

2. Experimental

2.1. Materials and methods

Pure $BiFeO_3$ and La doped $BiFeO_3$ (BFO) have been synthesized through sol-gel combustion method, urea as a fuel, using $Bi(NO_3)_3.5H_2O$, $Fe(NO_3)_3.9H_2O$. $La(NO_3)_3$ was added by $La_xBi_{1-x}FeO_3$ with x = 0.05 composition along with the pure $BiFeO_3$. Deionized water (DI) has been used during all preparation stages. For pure $BiFeO_3$ nanoparticles, $Bi(NO_3)_3.5H_2O$ and $Fe(NO_3)_3.9H_2O$ were dissolved separately in the DI, mixed then kept under vigorous stirring for

1 hour at RT in order to obtain a homogenous clear solution. After that, urea solution was added slowly in drops to the above solution for several hours until a very clear solution was obtained. The latter was introduced into a silica crucible then subjected to irradiated at a frequency of 2.54 GHz at 950 W output power for 10 minutes using a domestic microwave oven. The obtained solid powder was subsequently dried in a hot air oven at 70°C for 1 h, grounded in a mortar pestle and washed with ethanol and used for further studies. Similar process was followed for the preparation of $La_{0.05}Bi_{0.95}FeO_3$ nanoparticles.

2.2. Characterizations

The structural analysis by X-ray diffraction (XRD) was performed using a high resolution Rigaku – Uttima IV diffractometer equipped with CuKα radiation source (λ = 1.5418 Å). Rietveld refinement was analyzed by PDXL program. FTIR was studied using 4000-400cm^{-1} range of Perkin Elmer infrared spectrophotometer. HR-SEM analysis carried by VEGA 3 TESCAN and EDX was fiend out by Brucker Nano. Morphological observations were checked by high resolution transmission electron microscopy (TEM) using JEOL 2000 EX operating at 200 kV. Magnetic measurements were performed at room temperature by using vibrating sample magnetometer (VSM) PMC Micro Mag 3900 equipped with 1 Tesla magnet and a resolution of 0.5 μemu.

3. Results and discussion

3.1. Powder XRD analysis

Powder XRD patterns of $BiFeO_3$ (BFO) and $La_{0.05}Bi_{0.95}FeO_3$ (LBFO) nanoparticles were illustrated in Fig. 1. The samples were found to be as a well crystallized single $BiFeO_3$ phase (rhombohedrally distorted perovskite structure with the space group R3c). The XRD patterns of BFO and LBFO nanoparticles reveal peaks that can be assigned to the standard card of BFO perovskite structure (JCPDS card No. 86-1518). The two diffraction peaks around 2θ~32° existed due to high lanthanum concentration. In other rare earth element substitution, these two peaks are merged into a one extended peak. However, in LBFO, two peaks remain confirms that there is no phase transformation from rhombohedral to orthorhombic or monoclinic structures [19, 20]. The average particle size has been calculated by Scherrer's formula,

$$d=k\lambda/\beta\cos\theta$$

where

d = Thickness of the sample,

λ = 1.5406 Å which is the wavelength of X-ray source tube as Cu-Kα1 radiation

k = Dimensionless shape factor which is generally consider 0.9 for spherical particles,

θ = Bragg angle

β = Full width at half maxima (FWHM)

The calculated average crystallite size of particles of BFO and LBFO were found to be 18.9 and 17.1 nm respectively.

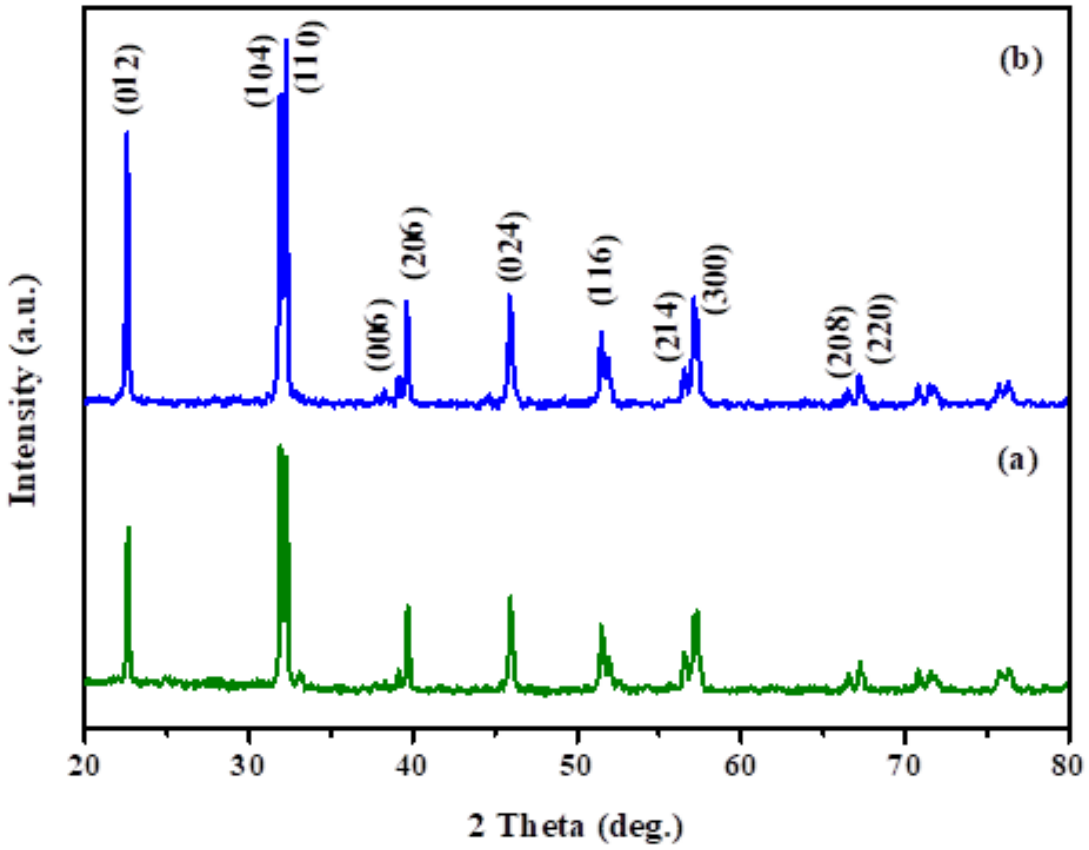

Figure 1. XRD patterns of (a) $BiFeO_3$ and (b) $La_{0.05}Bi_{0.95}FeO_3$ nanoparticles

3.2. FT-IR Analysis

The FT-IR spectra of the $BiFeO_3$ and $La_{0.05}Bi_{0.95}FeO_3$ nanoparticles were measured and shown in Fig. 2. The formation of perovskite structure can be confirmed by the presence of metal–oxygen band .The metal–oxygen bands at 570 (mode of stretching vibrations along the Fe–O axis) and 450 cm^{-1} (mode of the Fe–O bending vibration) in BFO and LBFO confirmed the presence of

octahedral FeO_6 groups in the perovskite compounds [21,22]. The broad band between 3,500 and 3,000 cm^{-1} was attributed to the antisymmetric and symmetric stretching of bond H_2O and OH^{-1} groups which may be due to the absorption of water molecules from the air, while peaks at 1600–1700 cm^{-1} correspond to nitrile (C ≡ N) [23].

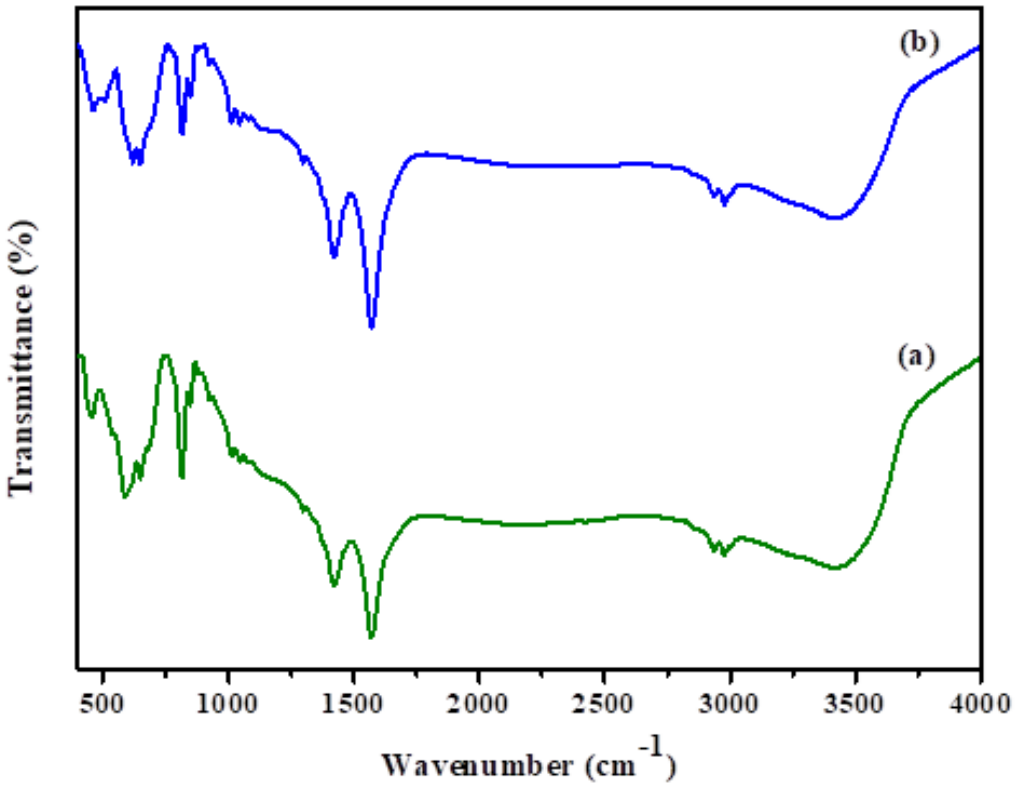

Figure 2. FT-IR patterns of (a) $BiFeO_3$ and (b) $La_{0.05}Bi_{0.95}FeO_3$ nanoparticles

3.3. Optical Properties

In order to study the optical characteristic of as-prepared BFO and LBFO, UV-Vis spectra were recorded in the range of 300–800 nm and shown in Fig. 3. It can be clearly seen that for all samples, the absorption was exhibited in the visible wavelength range (500–650 nm) suggesting their potential applications as visible-light-driven photocatalysts. The optical band gap was also calculated using Tauc's relation [24],

$$(\alpha h\nu)^2 = K(h\nu - Eg),$$

Where, α - absorbance, K –constant, Eg - optical band gap and hν - photon energy

The results indicated that the energy band gap (Eg) of BFO and LBFO were found to be 2.58 eV and 2.53 eV respectively. The estimated optical bandgap values for the LBFO nanoparticles was observed to increase with increasing the La doping concentration.

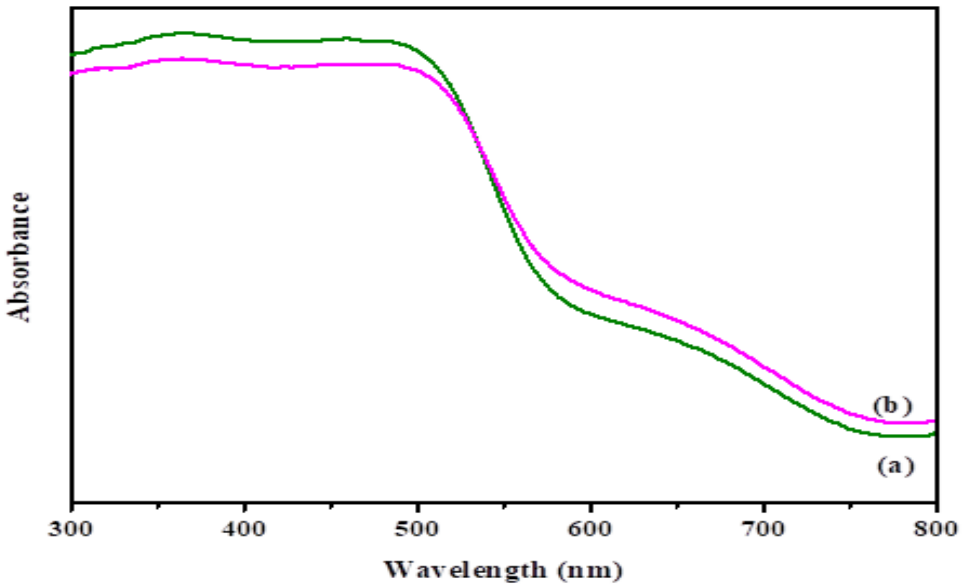

Figure 3. UV-Visible absorption spectra of (a) $BiFeO_3$ and (b) $La_{0.05}Bi_{0.95}FeO_3$ nanoparticles

3.4. Morphology studies

Fig. 4a, b shows the HR-SEM images of as synthesized $BiFeO_3$ and $La_{0.05}Bi_{0.95}FeO_3$ nanoparticles respectively. From Fig. 5 it as clear that the morphologies of the LBFO associated with the quantity of lanthanum doping. The $BiFeO_3$ particles had spherical shape with the average diameter of 19nm with rough surfaces as shown in Fig.4a,b. When La ions were doped, the particles still retained the sphere-like shape but the average diameters of particles decreased to 17nm with smoother surface. Hence, La doping played a vital role in the morphologies and dimensions of the BLFO.

e-ISSN 2320 –7876 www.ijfans.org
Vol.11, Iss.9, Dec 2022

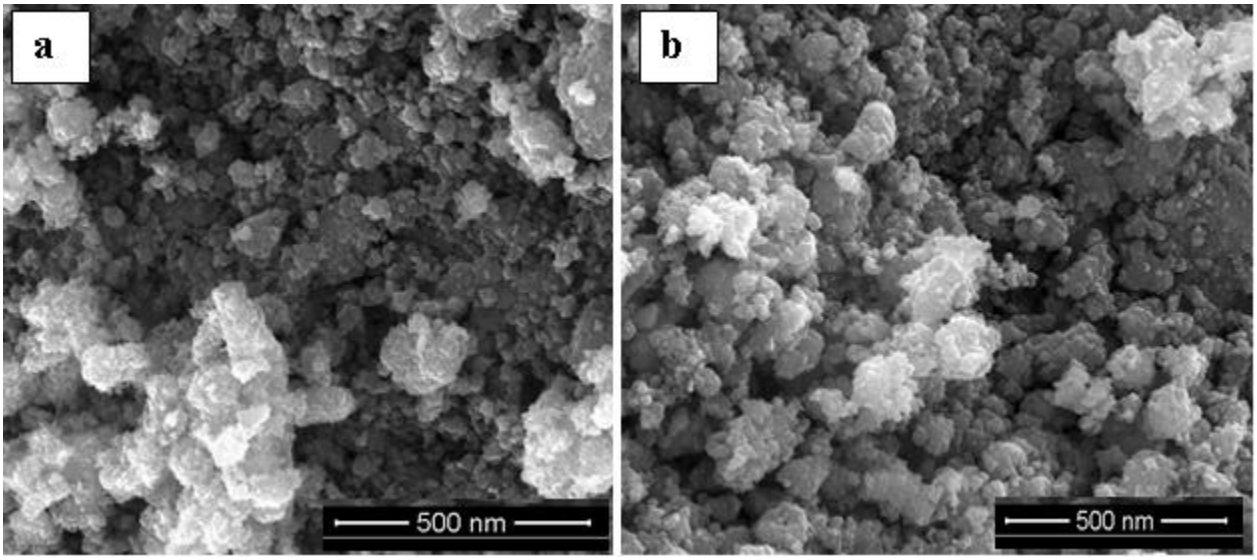

Figure 4. HR-SEM images of (a) $BiFeO_3$ and (b) $La_{0.05}Bi_{0.95}FeO_3$ nanoparticles

3.5. Magnetic properties

Fig. 5a,b shows magnetic hysteresis curve of $BiFeO_3$ and La doped $BiFeO_3$ nanoparticles respectively. It was clear that La doping had significant effect on the ferromagnetic properties of BFO nanoparticles. From the Figure it was observed that the ferromagnetic nature of pure $BiFeO_3$ nanoparticles increases as lanthanum was incorporated into the host lattice. The substitution of Bi^{+3} ions with La^{3+} ions suppress the spiral arrangement of spins so that magnetic moment increases. Another possible cause for the enhanced magnetic moment may incorporated with the increase of Fe^{+2} cations and oxygen vacancies.

Furthermore, the gradual change in crystal symmetry from R3c to Pnma might result in the progressive destruction of the cycloid coupling of spins by changing the canting angle andhence resulting increased net magnetization. In addition, at higher La doping concentrations, the grain sizes were observed to be smaller than those of the cycloid spin periodicity of the pure BFO structure (62 nm) which resulted in net magnetization when canted. These results suggested that the magnetic properties of BFO nanoparticles can be enhanced by La doping [25,26].

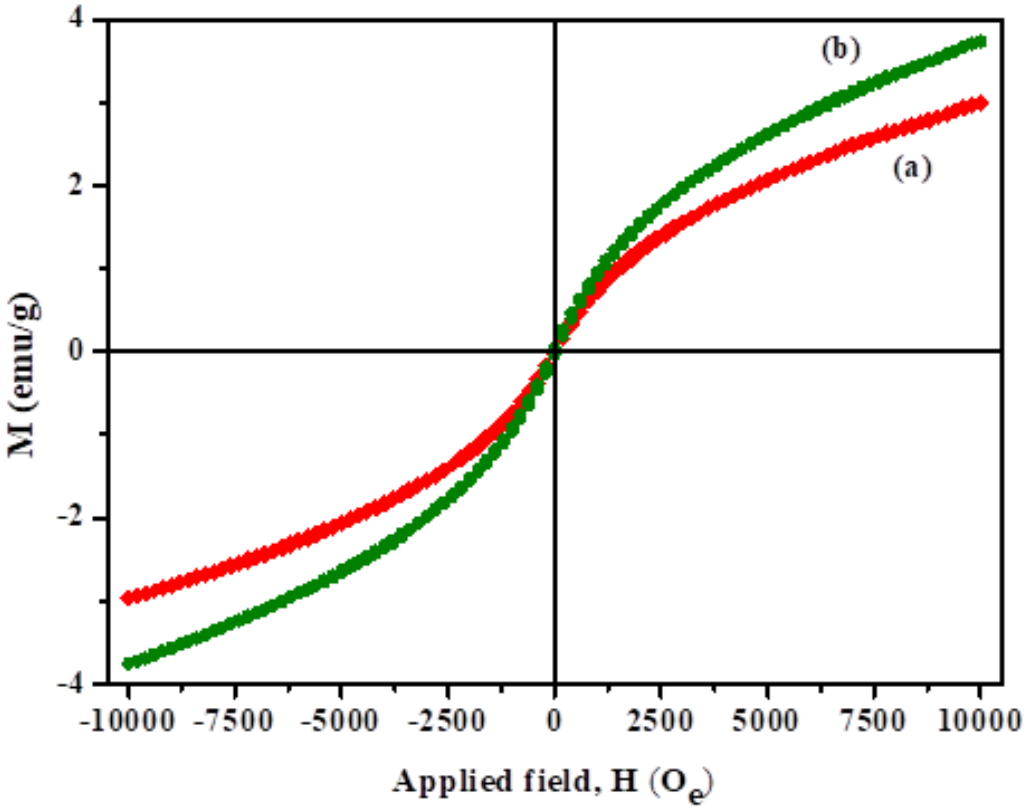

Figure 5. VSM analysis of (a) $BiFeO_3$ and (b) $La_{0.05}Bi_{0.95}FeO_3$ nanoparticles

4. Conclusions

Nanostructured $BiFeO_3$ (BFO) and $La_{0.05}Bi_{0.95}FeO_3$ (LBFO) samples were synthesized using urea as a fuel via sol-gel combustion method. The synthesized materials were analyzed by XRD, FT-IR, UV-Vis. spectroscopy, HR-SEM, HR-TEM, Magnetic measurements and antimicrobial studies. XRD of BFO demonstrates the rhombohedrally distorted perovskite structure with the space group R3c. The average particle size of BFO and LBFO were found to be 19 and 17nm respectively. The HR-SEM images of BFO and LBFO revealed the formation of sphere shaped nanostructures with uniform grain size. Also, it was found that the grain size was decreased by doping La contents to BFO. The magnetic measurements showed a ferromagnetic behavior of LBFO and the saturation magnetization drops drastically from 7 emu/g for $BiFeO_3$ up to 6 emu/g. The antibacterial investigation of BFO and LBFO exhibited excellent antibacterial activity against various Gram-positive and Gram-negative bacterial strains.

References

1. X. F.Hao, A. Stroppa, P.Barone, A.Filippetti, C.Franchini, S.Picozzi, Structural and Ferroelectric Transitions in Magnetic Nickelate $PbNiO_3$. New J. Phys. 16(2014), 015030-015050.
2. J.Wang, J.B.Neaton, H. Zheng, V. Nagarajan, S.B.Ogale, B. Liu, D. Viehland, V. Vaithyanathan, D.G. Schlom, U.V. Waghmare, Epitaxial $BiFeO_3$ Multiferroic Thin Film Heterostructures. Science 2003, 299, 1719−1722
3. Qiuhong Tan, Qianjin Wang, Yingkai Liu, Magnetic Properties and Spontaneous Polarization of La-, Mn- and N-Doped Tetragonal $BiFeO_3$: A First-Principles Study, Materials 11(2018), 985
4. G. Catalan, J.F. Scott, Physics and applications of bismuth ferrite. Adv. Mater. 21(2009) 2463-24853.
5. V.V. Lazenka, A.F. Ravinski, I.I. Makoed, J.Vanacken, G. Zhang, V.V. Moshchalkov, Weak ferromagnetism in La-doped $BiFeO_3$ multiferroic thin films. J. Appl. Phys. 111(2012), 123916- 1-4
6. J.C. Yang, Q. He, P. Yu, Y.H. Chu, $BiFeO_3$ thin flms: a play- ground for exploring electric-feld control of multifunction- alities. Ann. Rev. Mater. Res. 45(2015), 249–275.
7. P. Thilagavathi, A. Manikandan, S. Sujatha, S. K. Jaganathan, S. Arul Antony, Sol-gel synthesis and characterization studies of $NiMoO_4$ nanostructures for photocatalytic degradation of methylene blue dye, Nanoscience and Nanotechnology Letters, 8 (2016) 438-443.
8. P.Li, Y.H. Lin, C.W. Nan, Effect of nonmagnetic alkaline-earth dopants on magnetic properties of $BiFeO_3$ thin films. J. Appl. Phys. 110(2011), 033922
9. N.H.Hong, N.T. Huong, T.Y. Kim, S. Goumri-Said, M.B. Kanoun, M.B. Tuning magnetic properties of $BiFeO_3$ thin films by controlling rare-earth doping: Experimental and first-principles studies. J. Phys. Chem. C, 119(2015), 14351–14357.
10. L.Bi, A.R. Taussig, H.S. Kim, L. Wang, G.F. Dionne, D. Bono, K. Persson, G. Ceder, C.A. Ross, Structural, magnetic, and optical properties of $BiFeO_3$ and Bi_2FeMnO_6 epitaxial thin films: An experimental and first-principles study, Phys. Rev. B, 78(2008), 104106:1–104106:10.

11. P. Thilagavathi, A. Manikandan, S. K. Jaganathan, S. Arul Antony, J. Hameed Hussain, Photocatalytic activity, morphological and magneto-optical characterization studies of $CoMoO_4$ nanoparticles prepared by sol-gel method, Advanced Science, Engineering and Medicine, 9 (2017) 229-234.
12. E. M. Choi, S. Patnaik, E. Weal, S.L. Sahonta, G. Mecklenburg, H. Wang, Z. Bi, J. Xiong, M.G. Blamire, Q.X. Jia, Strong room temperature magnetism in highly resistive strained thin films of $BiFe_{0.5}Mn_{0.5}O_3$, Appl. Phys. Lett. 2011, 98, 012509:1-012509:3.
13. M. Maria Lumina Sonia, S. Anand, V. Maria Vinosel, M. Asisi Janifer, S. Pauline, A. Manikandan, Effect of lattice strain on structure, morphology and magneto-dielectric properties of $NiGd_xFe_{2-x}O_4$ ferrite nano-crystallites synthesized by sol-gel route, Journal of Magnetism and Magnetic Materials, 466 (2018) 238-251.
14. Q.J.Wang, Q.H. Tan, Y.K.Liu, First-principles study on ferromagnetism in Mn-doped tetragonal $BiFeO_3$. Comput. Mater. Sci.,105(2015), 1–5.
15. Nguyen Hoa Hong, Ngo Thu Huong, Tae-Young Kim , Souraya GoumriSaid , and Mohammed Benali Kanoun, Tuning Magnetic Properties of $BiFeO_3$ Thin Films by Controlling Rare-Earth Doping: Experimental and First-Principles Studies, The Journal of Physical Chemistry C,119(2015),14351–14357.
16. Lee, Y.H.; Wu, J.M.; Lai, C.H. Influence of La doping in multiferroic properties of $BiFeO_3$ thinfilms. Appl. Phys. Lett.,88(2006), 042903:1-042903:3.
17. Md. Mojahid Roni, Karimul Hoque, Tapash Chandra Paul, M.N.I.Khan, Md. Emran Hossain, Synthesis of La-doped $Mn_{0\cdot6}Zn_{0.4}La_xFe_{2-x}O_4$ and the study of its structural, electrical and magnetic properties for high frequency applications, Results in Materials,11(2021) 100215
18. K. Anandalakshmi, J. Venugobal , V. Ramasamy, Characterization of silver nanoparticles by green synthesis method using Pedalium murex leaf extract and their antibacterial activity, Applied Nanoscience 6(2016), 399–408
19. A.Chaudhuri, K. Mandal, Enhancement of ferromagnetic and dielectric properties of lanthanum doped bismuth ferrite nanostructures, Mater. Res. Bull., 47 (2012) 1057-1061.
20. Y. Slimani, M. A. Almessiere, A. D. Korkmaz, A. Baykal, A. Manikandan, H. Gungunes, M. S. Toprak, Ultrasound-assisted synthesis and magnetic investigations of

$Ni_{0.4}Cu_{0.4}Zn_{0.2}Ga_xGd_xFe_{2-2x}O_4$ ($0.00 \leq x \leq 0.04$) nanosized spinel ferrites, Applied Physics A 128 (2022) 1-14..

21. M. Sertkol, Y. Slimani, M.A. Almessiere, H. Sozeri, R. Jermy, A. Manikandan, S.E. Shirsath, A. UI-Hamid, A. Baykal, Sonochemical synthesis of $Mn_{0.5}Zn_{0.5}Er_xDy_xFe_{2-2x}O_4$ ($x \leq 0.1$) spinel nanoferrites: Magnetic and textural investigation, Journal of Molecular Structure, 1258 (2022) 132680.
22. M. P. Mani, A. A. M. Faudzi, S. Mohamaddan, A. F. Ismail, R. Rathanasamy, A. Manikandan, S. K. Jaganathan, Engineered polymer matrix novel biocompatible materials decorated with eucalyptus oil and zinc nitrate with superior mechanical and bone forming abilities, Arabian Journal of Chemistry, 104079 (2022).
23. M. A. Almessiere, S. Güner, Y. Slimani, A. Baykal, S. E. Shirsath, A. D. Korkmaz, R. Badar, A. Manikandan, Investigation on the structural, optical, and magnetic features of Dy^{3+} and Y^{3+} co-doped $Mn_{0.5}Zn_{0.5}Fe_2O_4$ spinel ferrite nanoparticles, Journal of Molecular Structure 1248, 131412 (2022).
24. M. Sertkol, S. Güner, M. A. Almessiere, Y. Slimani, A. Baykal, H. Gungunes, E. M. Alsulami, F. Alahmari, M. A. Gondal, S. E. Shirsath, A. Manikandan, Effect of Bi^{3+} ions substitution on the structure, morphology, and magnetic properties of Co-Ni spinel ferrite nanofibers, Materials Chemistry and Physics, 284 (2022) 126071.
25. M. A. Almessiere, Y. Slimani, N. A. Algarou, M. A. Gondal, Y. S. Wudil, M. Younas, I. A. Auwal, A. Baykal, A. Manikandan, Electrospinning synthesis of Cd substituted Ni-Co spinel ferrite nanofibers: An investigation on their structural and magnetic features, Applied Physics A, 127 (2021) 785,
26. M. A. Almessiere, Y. Slimani, N. A. Algarou, M. A. Gondal, Y. S. Wudil, M. Younas, I. A. Auwal, A. Baykal, A. Manikandan, Investigation on electrical and dielectric properties of hard/soft spinel ferrite nanocomposites of $CoFe_2O_4/(NiSc_{0.03}Fe_{1.97}O_4)x$, Vacuum, 194 (2021) 110628,